

Calculation of the atmospheric neutrino flux improved with recent cosmic ray observations

M. Honda¹, T. Kajita¹, K. Kasahara², and S. Midorikawa³

¹Institute for Cosmic Ray Research, University of Tokyo, Kashiwa-no-Ha, Chiba 277-8582, Japan

²Shibaura Institute of Technology, Fukasaku, Ohmiya, Saitama 330-8570, Japan

³Faculty of Engineering, Aomori University, Aomori 030-0943, Japan.

Abstract. The primary cosmic ray spectrum below 100 GeV has been measured very accurately by the recent experiment, such as BESS and AMS. Also the measurements of secondary cosmic rays such as muons and gamma rays are extensively carried out in order to improve the prediction of atmospheric neutrino flux. Using the results of accurately measured cosmic ray fluxes, we revise the hadronic interaction model and calculate the atmospheric neutrino flux.

1 Introduction

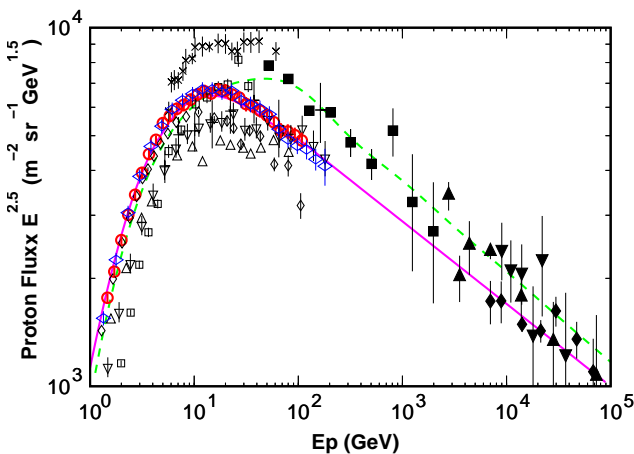


Fig. 1. Primary cosmic ray observation and model curves for proton cosmic rays. Pluses, closed squares, closed vertical diamond, closed upward triangles, and closed downward triangles are from Refs.[22],[26],[25],[34],[35],[36], and [38] of Honda et al., 1995, respectively. Crosses, open squares, open upward triangles, open downward triangles, open vertical diamonds, open circles BESS, and open horizontal diamonds are from Refs, [18],[19],[20],[21],[22],[23], and [24] of Honda et al., 2001, respectively. The solid line shows the proton flux model used in this paper and dashed line the one used in Honda et al., 1995.

Correspondence to: M. Honda (mhonda@icrr.u-tokyo.ac.jp)

After we have had presented a calculation of the atmospheric neutrino flux (Honda et al., 1995, referred as HKKM hereafter.), the measurement of the primary cosmic ray observation has been improved in the accuracy. Especially the agreement of proton flux by the BESS and AMS within $\sim 5\%$ is a milestone in the cosmic ray physics (Fig. 1). However, it is $20 \sim 25\%$ lower than the proton flux model used in the HKKM calculation. The new compilation of the primary cosmic ray spectrum is reported in another paper of this conference (Gaisser et al., 2001), and we use the “high” fit parameterization in the paper.

There have been improvements in the hadronic interaction model in the high energy physics. In the HKKM calculation, we used the NUCRIN for $\leq E_{lab} \leq 5$ GeV, FRITIOF version 1.6 for $5 \text{ GeV} \leq E_{lab} \leq 500$ GeV, and an original code developed by one of our author (Kasahara, 1995) was used above 500 GeV. We simply refer the combination of the hadronic interaction models as the HKKM interaction model. In this paper, we also study dpmjet3 (Roesler, 2000) from the modern hadronic interaction models, and compare the resulting muon spectrum with the experimental data, as well as the results of HKKM interaction model.

Note that the measurements of the secondary cosmic rays, such as atmospheric muons and gamma rays, have been carried out extensively to improve the prediction of atmospheric neutrino flux (Boezio et al., 2000) (Motoki et al., 2001) (Sanuki et al., 2001). The accurately measured primary and secondary cosmic ray fluxes enable us to calibrate the calculation method including the hadronic interaction model. A similar study with the atmospheric gamma ray has been done in a separate paper of this conference (Kasahara et al., 2001).

2 Comparison of HKKM and dpmjet3 interaction models

We have plotted the x-distribution of $P + Air \rightarrow P + X$ and $P + Air \rightarrow \pi + X$ calculated with the dpmjet3 interaction model in Fig. 2, and those with HKKM interac-

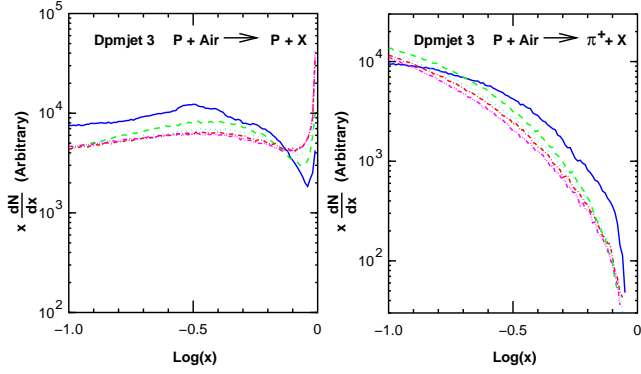


Fig. 2. X-distribution of $P + Air \rightarrow P + X$ (left), and $P + Air \rightarrow \pi^+ + X$ (right) calculated with the dpmjet3 interaction model. Solid lines stands for the input kinetic energy of 10 GeV, dashed lines for 100 GeV dotted lines for 1 TeV, dash dot for 10 TeV, and dash dot dot for 100 TeV.

tion model in Fig. 3. The variable x is defined here as $x = E_{kinetic}^{secondary} / E_{kinetic}^{projectile}$.

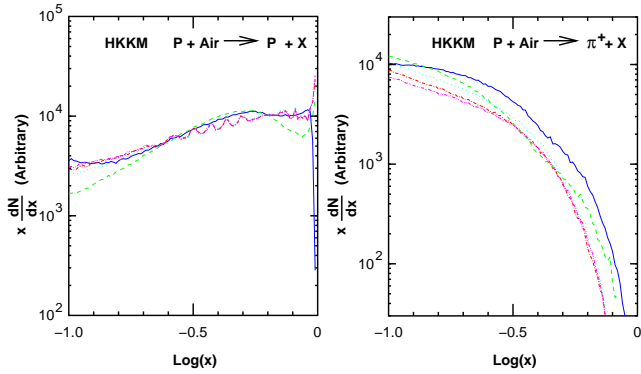


Fig. 3. X-distribution of $P + Air \rightarrow P + X$ (left), and $P + Air \rightarrow \pi^+ + X$ calculated with the HKKM interaction model. Solid lines stands for the input kinetic energy of 10 GeV, dashed lines for 100 GeV dotted lines for 1 TeV, dash dot for 10 TeV, and dash dot dot for 100 TeV.

The secondary spectrum of pions are a little harder in dpmjet3 interaction model. The secondary spectrum of protons for dpmjet3 has a dip at $\log(x) \sim -0.1$ which is not seen in HKKM model. As the results of these differences, pions carry $\sim 15\%$ large energy fraction in the dpmjet3 hadronic interaction model than the HKKM hadronic interaction model. The nucleons, however, carries ~ 20 smaller energy fraction in the hadronic interaction dpmjet3 than the HKKM hadronic interaction model.

3 Energy relation of atmospheric neutrinos and muons to primary cosmic rays

Before starting the study of atmospheric muon spectra, it is useful to see the energy relation between the primary cosmic rays and atmospheric neutrinos and muons. Fig. 4 shows the energy distribution of primary cosmic rays which produce

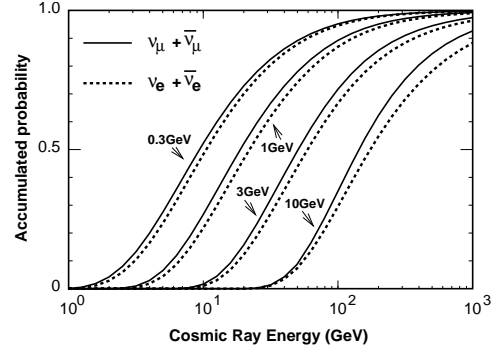


Fig. 4. The energy distributions of primary cosmic rays which produce 0.3, 1, 3, and 10 GeV atmospheric neutrinos in the accumulated probability. They are calculated for low rigidity cutoff site and for near vertical directions. The Solid lines are for $\nu_\mu + \bar{\nu}_\mu$ and dotted lines for $\nu_e + \bar{\nu}_e$.

0.3, 1, 3, and 10 GeV atmospheric neutrinos in the accumulated probability. We note that the median energy of relevant cosmic ray for those neutrinos are around 8, 20, 50, and 140 GeV, respectively

In Fig. 5, the energy distribution of cosmic rays which produce 0.3, 1, 3, and 10 GeV/c atmospheric muons at the ground level and for near vertical directions. The median energy of the relevant primary cosmic rays are around 20, 30, 50, 110 GeV respectively. The energy distribution of relevant primary cosmic ray for muons is closer than that for neutrinos and have wider overlaps for different muon momentums.

In Fig. 6, the energy distribution of primary cosmic rays which produce 0.3, 1, 3, and 10 GeV/c atmospheric muons at the air depth of 4.6 g/cm^2 . The median energy of the relevant primary cosmic rays are around 4, 7, 20, 60 GeV respectively. Note that while the energy of relevant primary cosmic ray is lower than that for muons at ground level the separation of energy distribution is better at balloon altitude. These are great advantages to test the interaction models.

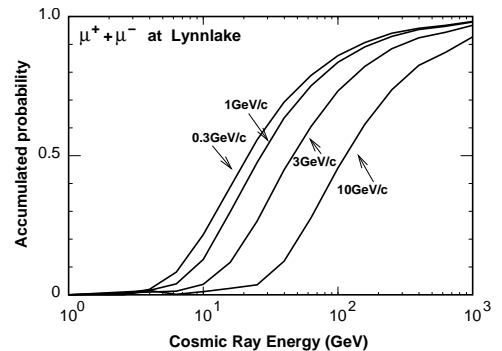


Fig. 5. The energy distribution of primary cosmic ray which produce 0.3, 1, 3, and 10 GeV/c atmospheric muons at low cutoff rigidity site in the accumulated probability.

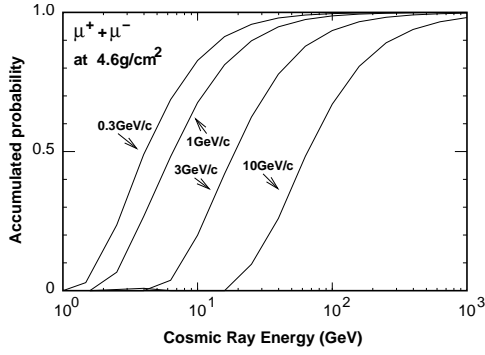


Fig. 6. The energy distribution of primary cosmic ray energy which produce 0.3, 1, 3, and 10 GeV/c atmospheric muons at the balloon height (air depth of 4.6 g/cm²), in the accumulated probability.

4 Muons at the ground level

In Fig. 7, we show the muon flux observed by BESS group and calculated ones with dpmjet3 and HKKM interaction models for very low rigidity cutoff site (Lynnlake $R_g \ll 1$ GV) and for near vertical directions. In the right panel of Fig. 7, the ratio to the calculation with dpmjet3 interaction model is shown to magnify the differences.

From the ratio figure, it is seen that the fluxes calculated with HKKM interaction model disagree with the observation below ~ 3 GeV. On the other hand the calculated fluxes with dpmjet3 marginally agree with the observation. At ~ 10 GeV/c region, the agreement of HKKM model and observation becomes better, but the error and the scatter of data points are large. There we conclude that HKKM interaction is disfavored by the observed muon flux below ~ 3 GeV. This muon energy region corresponds to the primary energy of 10 – 100 GeV from Fig. 5.

5 Muons at mountain altitude

In Fig. 8, we show the muon flux observed by BESS group at Mt. Norikura (2770m a.s.l.) and the calculated ones for this altitude and for near vertical directions. In the right panel

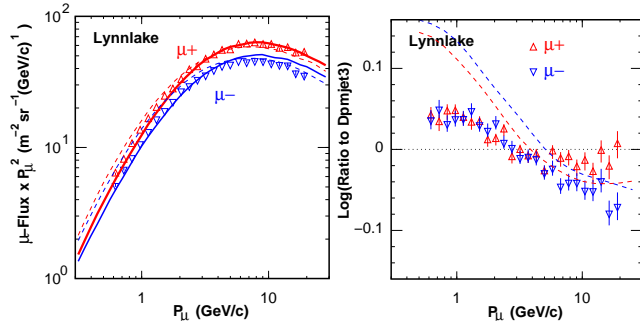


Fig. 7. Observed and calculate muon fluxes for Lynnlake (left) and the ratios to the calculation with dpmjet3 model (right). Solid lines show the calculated flux with dpmjet3, and dashed line show the calculated flux with HKKM interaction model.

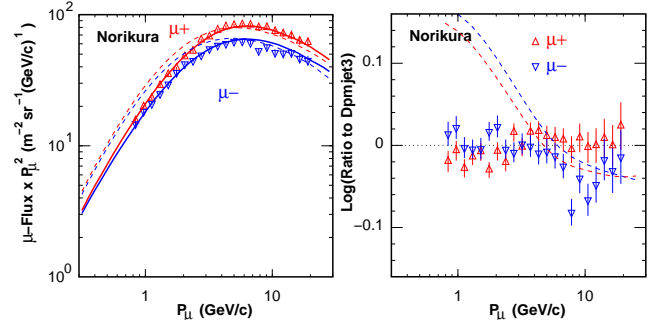


Fig. 8. Observed and calculate muon fluxes for Mt Norikura (left) and the ratios to the calculation by dpmjet3 model (right). Solid lines show the calculated flux by dpmjet3, and dashed line show the calculated flux by HKKM interaction model.

of Fig. 8, the ratio to the calculation by dpmjet3 interaction model is shown to magnify the differences.

The agreement between the calculated flux with dpmjet3 interaction model and observed one is remarkable. Except for μ^- flux at ~ 10 GeV/c, the agreement is within $\sim 5\%$. The energy of the relevant primary cosmic rays at mountain altitude is similar to that at ground level, but a little lower. Thus the muon observation at mountain altitude supports dpmjet3 in the energy region around 9 – 90 GeV in the primary cosmic ray energy. On the other hand, the calculated results by HKKM model does not agree with the observed data except for the ‘crossing points’ at ~ 5 GeV/c.

6 Muons at balloon altitude

In Fig. 9, we show the muon fluxes observed by BESS (Sanuki et al., 2001) at the air depth of 4.6 g/cm², and by CAPRICE (Boezio et al., 2000) at the air depth of 3.9 g/cm², with the calculated ones. Also the ratios to the calculated muon fluxes by dpmjet3 are shown altogether in Fig. 10. Although, the error and the scatter of data points are large, it is seen that dpmjet3 is preferred from the observed data at muon energies > 1 GeV/c. However, a large statistics is not available at this altitude, due to the small flux itself and the limited observation time. Therefore, it is not yet convincing.

7 Summary and Atmospheric neutrino flux

In the comparison of observed flux and calculated ones, we have seen that dpmjet3 shows better agreements than the HKKM interaction model at all the altitude level, and corresponding to the primary cosmic ray energy range of 7–100 GeV.

Using the dpmjet3 and the new flux model, we have calculated the atmospheric neutrino flux and show in Fig. 11 as well as the ones calculated with HKKM interaction model and new flux model. We find dpmjet3 gives $\sim 15\%$ lower neutrino fluxes below ~ 1 GeV, but gives $\sim 10\%$ higher flux at ~ 10 GeV. The atmospheric neutrino flux calculated with the dpmjet3 hadronic interaction model may be a little more

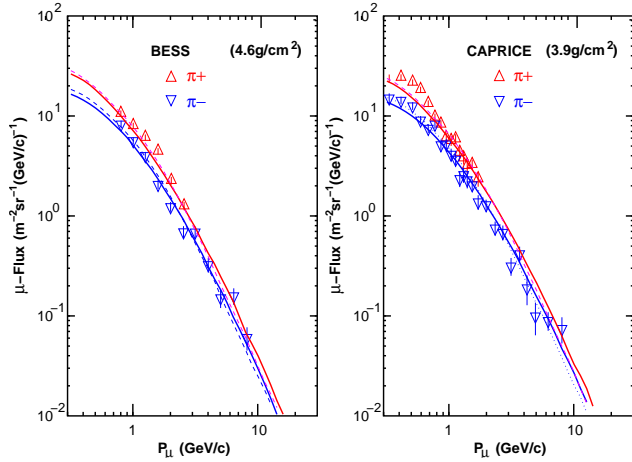


Fig. 9. Muon fluxes observed at the balloon altitude by BESS(4.6 g/cm²) (Sanuki et al., 2001) and CAPRICE(3.9 g/cm²) (Boezio et al., 2000) experiments. The solid lines show the calculated muon flux by the dpmjet3, and dashed lines by HKKM interaction model for each panel.

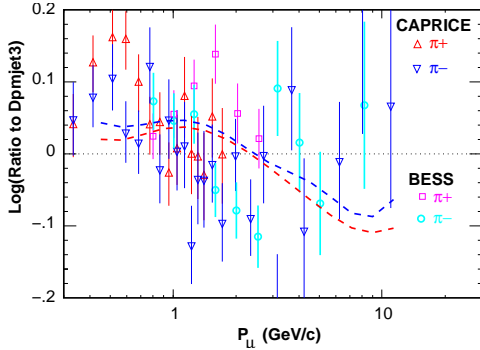


Fig. 10. Ratio of muon fluxes to the calculate one by dpmjet3 interaction model. The dashed lines show the calculated fluxes by the HKKM interaction model.

reliable than that calculated with the HKKM hadronic interaction model below $\lesssim 3$ GeV.

We have presented the study of interaction model using the accurately measured secondary cosmic ray fluxes, and find that it is useful. However, we have to stress that the study is still progressing. Note that the accuracy of the primary cosmic ray spectrum is crucial in this study. Also We need more observed data, especially the muon flux at mountain and balloon altitudes, to improve this study.

Acknowledgements. We are grateful to T.Sanuki and K.Motoki for muon data and discussions. We also thank to J.Nishimura and A.Okada for discussions.

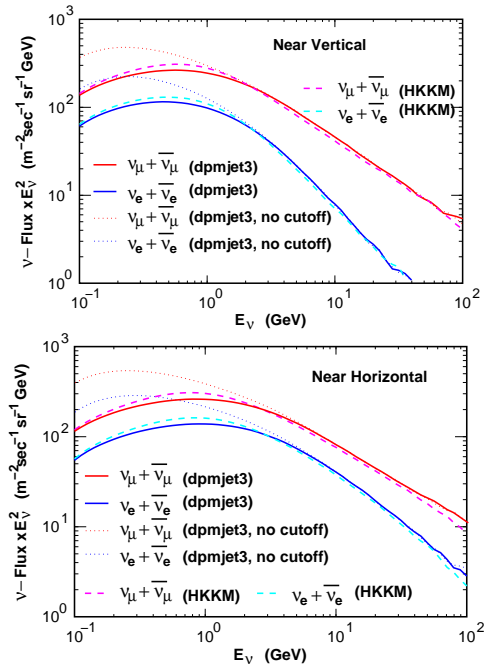


Fig. 11. Atmospheric neutrino fluxes calculated by the dpmjet3 and HKKM interaction models.

References

- Gaisser, T.K. et al., This conf.
 Honda, M. et al, Phys. Rev. D 54, 4985 (1995).
 Honda, M. et al., hep-ph/0103328 (2001).
 K. Kasahara, Proc. of the 24th ICRC, Rome. Vol. 1, 399 (1995). See also the World-Wide-Web address;
<http://eweb.b6.kanagawa-u.ac.jp/~kasahara/ResearchHome/cosmosHome/>.
 Roesler, S. Engel, R. and Ranft J., SLAC-PUB-8740, hep-ph/0012252, to be published in Proceedings of the the Conference “Monte Carlo 2000”, Lisbon, Portugal, 23-26 October 2000
 Boezio, M. et al., Phys. Rev. D 64, 032007-1 (2000).
 Motoki, K. et al., This conf.
 Sanuki, T. et al., This conf.
 K. Kasahara et al., This conf.